

Damage state evaluation of experimental and simulated bolted joints using chaotic ultrasonic waves

T. R. Fasel, M. B. Kennel and M. D. Todd*

University of California San Diego, La Jolla, CA 92093-0085, U.S.A.

E. H. Clayton

Quartus Engineering, San Diego, CA 92121-3771, U.S.A.

G. Park

Los Alamos National Laboratory, Los Alamos, NM 87545, U.S.A.

(Received August 19, 2008, Accepted September 21, 2008)

Abstract. Ultrasonic chaotic excitations combined with sensor prediction algorithms have shown the ability to identify incipient damage (loss of preload) in a bolted joint. In this study we examine a physical experiment on a single-bolt aluminum lap joint as well as a three-dimensional physics-based simulation designed to model the behavior of guided ultrasonic waves through a similarly configured joint. A multiple bolt frame structure is also experimentally examined. In the physical experiment each signal is imparted to the structure through a macro-fiber composite (MFC) patch on one side of the lap joint and sensed using an equivalent MFC patch on the opposite side of the joint. The model applies the waveform via direct nodal displacement and 'senses' the resulting displacement using an average of the nodal strain over an area equivalent to the MFC patch. A novel statistical classification feature is developed from information theory concepts of cross-prediction and interdependence. This damage detection algorithm is used to evaluate multiple damage levels and locations.

Keywords: structural health monitoring; bolted joint; active sensing; guided waves; AR model; information theory.

1. Introduction

One of the most common structural sub-systems used in design is the moment-resisting connection, often executed by threaded fastener assemblies. Threaded fasteners are popular due to advantages such as the ability to develop a clamping force and the ease with which they may be disassembled for maintenance or replacement. It is well known that such fasteners loosen under shock, vibration, or thermal loading, and a recent comprehensive discussion of these effects is given in (Hess 1998). A combined finite element and experimental study of dynamic shear load-induced loosening has even shown that the minimum load required to initiate loosening is lower than previously reported (Pai and Hess 2002). Because of the highly localized nature of bolt loosening and failure, most approaches in

*Corresponding Author, E-mail: mdt@ucsd.edu

this field have involved two- and three-dimensional finite element formulations (Bursi and Jaspart 1997, Bursi and Jaspart 1998, Pai and Hess 2002).

These model-based approaches have been well suited to studying the fundamental nature of the problem and guiding the design process, but they are not useful for in-situ joint assessment in the field. The most prevalent method currently employed in practical field applications for damage identification in structural joints is ultrasonic testing, especially in the aerospace industry (Guyott, *et al.* 1986). These ultrasonic waves have proven to be a useful tool for damage detection and localization because of the small length and time scales on which they operate. One such conventional ultrasonic bond inspection technique is known as the Fokker bond method. This ultrasonic inspection is executed in ground tests of aircraft and consists of measuring the frequency-dependent reflection coefficients of ultrasonic waves propagating through the bonded or jointed sub-structure in the megahertz frequency range (Guyott and Cawley 1988). This technique has been successfully implemented for some time, but it has several limitations that cause continuous in-situ structural health monitoring (SHM) to be infeasible. It is inherently an off-line technique, requires bulky test equipment and an expert technical operator, and has a very limited spatial inspection range. Some of the first continuous SHM monitoring techniques employed were global ones based on vibration testing and accelerometer response. However, these methods operate at frequencies too low (wavelengths too large) to be able to identify the small changes in joint preload loss that may need to be detected (Doebling, *et al.* 1996). Only significant bolt preload losses are typically detectable when vibration-domain techniques such as modal analysis are employed (Todd, *et al.* 2004).

This problem of damage localization for in-situ health monitoring has recently been addressed using guided ultrasonic waves (Alleyne, *et al.* 1996, Wilcox, *et al.* 1999). These guided waves are suitable for continuous monitoring because relatively few actuators/sensors need to be used by exploiting the waveguide geometry of the structure (plates, rails, bars, etc.). While some work has been done using guided waves created with air-coupled transducers (Castaings, *et al.* 1996, Tuzzeo and Lanza di Scalea 2001) or laser vibrometry (Staszewski, *et al.* 2004), these methods are difficult to implement for continuous health monitoring. Most researchers have turned to the use of piezoelectric actuators/sensors as an effective means of in-situ ultrasonic damage detection (Giurgiutiu and Zagari 2002, Wait, *et al.* 2004, Giurgiutiu 2005). Some of the most frequently employed SHM methods that use actively created high frequency guided waves to interrogate adhesively bonded joints are the examination of dispersion curves and attenuation coefficients (Xu, *et al.* 1990, Pilarski and Rose 1992, Seifried, *et al.* 2002) as well as reflection and transmission characteristics (Rokhlin 1991, Lowe and Cawley 1994). Many of these methods also apply the use of denoising and wavelet transforms to increase signal-to-noise ratio and to selectively examine individual mode propagation of sensed waveforms (Abbate, *et al.* 1997, Lanza di Scalea, *et al.* 2004). These techniques are well established and can work in certain structures with simple geometries (plates, beams, etc.) or on sections with constant cross-section properties in the wave propagation direction (rails). However, these methods cannot easily be applied to irregular geometries, such as bolted joints, because of mode conversion and wave interference effects that arise as a result of complex interfaces and mechanical impedance mismatches across the joint. Instead, some researchers have attempted to employ bulk insonification, where an ultrasonic source is excited and the resultant long-time, or diffuse, wave field is examined to identify structural changes (Michaels and Michaels 2005). This method is preferable to the standard guided wave method for structures with complex boundary conditions or geometries that make tracking and analysis of a single propagating mode difficult or impossible. For an overview of the ultrasonic health monitoring paradigm see Fig. 1. Fig. 2 shows the similarity between standard bonded connection testing and testing undertaken for bolted

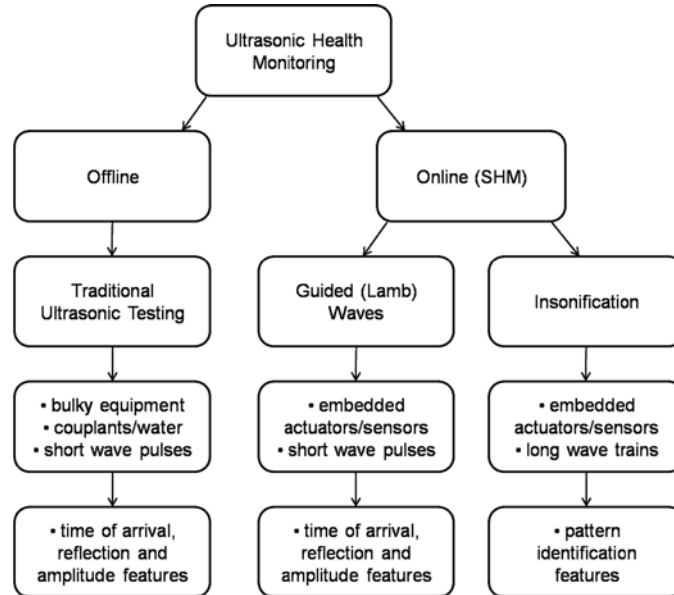


Fig. 1 Ultrasonic health monitoring paradigm

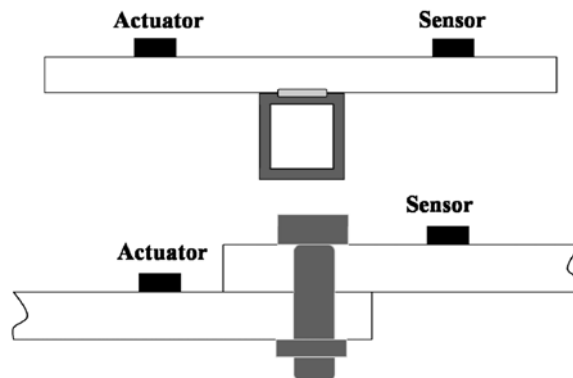


Fig. 2 Test configurations for standard bonded joints (top, short pulses) and bolted connections (bottom, long wavetrains) used in this study

connections.

Methods that employ chaotic excitations and attractor-based prediction error algorithms have demonstrated the capacity to detect bolt preload loss in various test bed structures with enhanced sensitivity over traditional vibration-domain analyses (Nichols, *et al.* 2003, Todd, *et al.* 2004). Unfortunately, these chaotic excitations are also low frequency in nature and are therefore unable to localize damage within a structure. More recent research uses the benefits of combining ultrasonic guided waves (small length and time scales) with chaotic excitations (which enable and enhance pattern recognition techniques) for damage detection of bolted connections via bulk insonification (Fasel, *et al.* 2005, 2006). This synthesis of techniques is accomplished by shifting the energy of a low-frequency chaotic process, such as the common Lorenz signal, into the ultrasonic frequency range (>20 kHz) and launching it into the structure as a guided wave. These chaotic ultrasonic waves (CUWs) are imparted to a structure by a

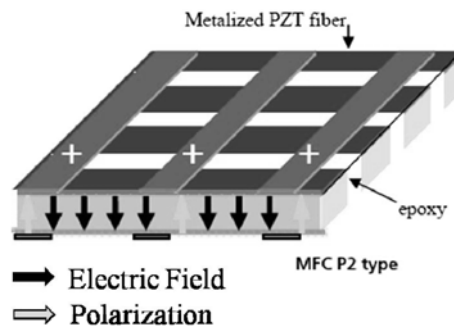


Fig. 3 Macro fiber composite (MFC) patch schematic

particular kind of piezoelectric actuator known as a Macro Fiber Composite (MFC) patch and do not require a large energy input into the system. An MFC patch is also used to acquire the vibration response in an active sensing manner. A schematic of an MFC patch can be seen in Fig. 3. The primary objective in this study is to extract a damage feature, whose basis is in coding theory, to statistically classify the level and location of preload loss in bolted joint assemblies. The objective is that the combination of chaotic ultrasonic insonification, pattern recognition, and a novel statistical classification scheme will result in a procedure that can be used for in situ SHM that does not require knowledge or modeling of complex structural geometry. Such in-situ SHM can provide expected economic or life-safety benefits in a number of applications where threshold-driven preload levels govern performance.

This paper is organized in the following way. Section 2 covers the theory and background necessary for the understanding of subsequent sections. Section 3 examines a three-dimensional finite element simulation designed to model the behavior of guided ultrasonic waves through a bolted lap joint connection. Section 4 details the results of two experiments that were created to ascertain the effectiveness of the investigated damage detection scheme. First, a single bolt lap joint that is configured in the same manner as the simulation is examined. Second, experiments performed on a multiple bolt frame structure will showcase the ability of this SHM method to correctly identify multiple damage levels and locations. A brief summary will then be offered in Section 5.

2. Theory and background

2.1. Signal creation

The chaotic ultrasonic waves are fundamentally created via amplitude modulation, i.e., by multiplying a single ultrasonic frequency tone by an amplitude envelope that is created by a chaotic process. The waveform appears as a narrowband, chaotically-modulated signal centered at the same central frequency as the original ultrasonic tone. For this study a carrier frequency of 80 kHz was chosen because of the relatively minor dispersion that occurs in aluminum at that frequency (although this is not a requirement), because of the bar thickness that is used in the experimental study, and because the traveling modes are well-separated in phase velocity space.

Creation of this signal is a multi-step process and starts with the generation of a 1 Hz sine wave with a timestep $dt = f_c/f_s$, where f_c is the frequency of the carrier wave and f_s is the sampling frequency which for this study is always 4 MHz. A chaotic signal can then be constructed using the output of the x

variable from the following three-dimensional nonlinear Lorenz system:

$$\begin{aligned} \dot{x} &= 10(y-x) \\ \dot{y} &= (-xz + 28x - y) \\ \dot{z} &= (xy - 8z/3) \end{aligned} \tag{1}$$

There is nothing special about the Lorenz system for generating chaotic output; any system capable of producing a chaotic output is suitable. Eq. (1) is integrated using a time-step $dt_{lorenz} = dt * R$, where R is a frequency ratio that can be modified to change the frequency of the chaotic signal. For this study we use a value of $R = 1/3$ which creates a signal in which the significant frequency information (as determined by a loss of 40 dB in power spectral density) is less than 1.5 Hz. A value of $R = 1/30$ would result in significant frequency information being less than 0.2 Hz. This chaotic signal is normalized through division by the maximum of the absolute value of the signal so that the values range from -1 to 1. A modulated signal is then created using the following equation:

$$y = \sin(2\pi * t) * (1 + d * x)$$

where x is the Lorenz waveform, $\sin(2\pi * t)$ is the originally created sine wave, d is the modulation depth, and y is the chaotically amplitude-modulated output signal. If the value of d , which controls signal bandwidth, is greater than one, the resulting signal will be over-modulated and will result in a phase inversion at the points where $|d * x| > 1$. These phase inversions would be detrimental to any prediction algorithm, and d is therefore restricted to the range $0 < d \leq 1$. The amplitude modulated signal

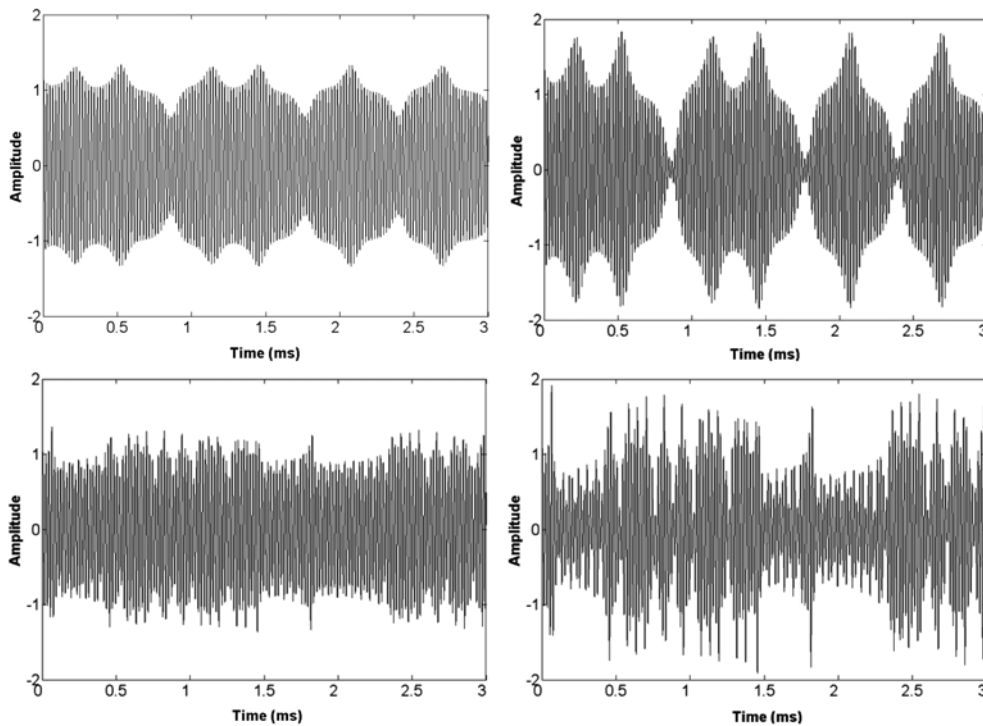


Fig. 4 Modulated signals using (a, top left) $R = 0.10$ and $d = 0.5$; (b, top right) $R = 0.10$ and $d = 1.0$; (c, bottom left) $R = 0.33$ and $d = 0.5$; (d, bottom right) $R = 0.33$ and $d = 1.0$

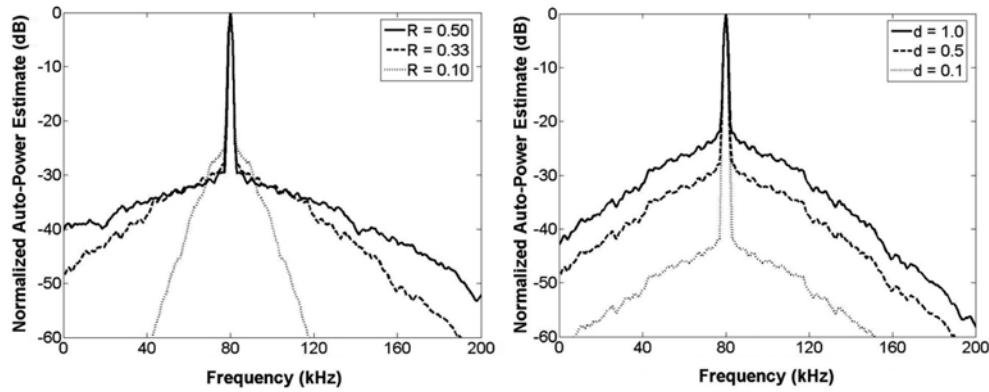


Fig. 5 (a, left) Power spectral density of modulated signals using $d = 0.5$; (b, right) Power spectral density of modulated signals using $R = 0.33$

is then upconverted to the target carrier wave frequency by multiplying $dt * f_c$. The resulting chaotic time series are also smoothed in time at its boundaries with a trapezoidal window to facilitate launching with piezoelectric devices. The CUWs were launched over a 2 ms time period. Fig. 4(a-d) depict the actual time series for various parameter combinations and Fig. 5(a-b) show the effect of changing the frequency ratio R as well as the modulation depth d on the power spectral density of the modulated sine wave. The effectiveness of the damage detection technique used in this study is highly dependent on carrier frequency and frequency ratio but appears to be relatively insensitive to modulation depth, provided a value significantly larger than zero is used (Fasel, *et al.* 2008).

2.2. Feature extraction

Once the CUW has been created it is then imparted to the structure through an MFC patch. The waveform then travels through the bolted joint and is detected by a second sensing MFC. The primary task at this point in the damage detection scheme is to decide what feature(s) from the measured waveform may be extracted to best assess the preload status of the joint. A novel statistical classification technique with its basis in information theory is employed for this study.

A fundamental theorem of Shannon's information theory says, described intuitively, "the best compression for any given data set comes from a codebook designed exactly for the statistics of that source, any other codebook will give worse results" (Shannon and Weaver 1949). For instance, if one has a codebook (e.g. taking language elements like words into shorter codes) consisting of English words and another consisting of French words etc., then a new time series of letters can be represented in the shortest compressed format when using the English codebook versus all others if the new text is, in fact, written in English. Compression performance is the classic text categorization methodology. Modern statistics has melded ideas of information theory to extend to continuous signals, where compression performance is intimately tied with out-of-sample prediction error, and a codebook is the model for a source (something that produces time series data). In this case the source arises from an actual physical process (the guided wave propagating through a bolted joint). This idea leads to a procedure for classifying time series using cross-prediction error, as literal "data compression" is not actually necessary, just its "virtual" performance. First, a suitable model of the measured response time series is required, as opposed to the computationally-intensive, first-principles physical spatially-extended finite element model of the joint.

The perfect model for classification is not needed, as it can work well with reasonable model misspecification. However, the better the underlying statistical model is, of course, the more the classification performance will improve.

The first step in this method employs the use of autoregressive (AR) models, which have previously been shown to be useful in damage classification schemes (Sohn and Farrar 2001, Sohn, *et al.* 2001). The discretely observed output time series $\mathbf{x}(n)$ is modeled with an AR model of the form

$$\mathbf{x}(n) = \sum_{i=1}^p \alpha_i \mathbf{x}(n-i) + \mathbf{e}(n) \quad (3)$$

where p is the order of the AR model with associated coefficients α_i and residual error $\mathbf{e}(n)$. In this study it was determined that an order of $p = 25$ effectively models the sensed waveforms. The AR coefficients are estimated through minimization of the sum of squared forward prediction errors (Brockwell and Davis 1991). All signals are normalized by dividing the standard deviation of the signal before use of the AR model.

The process behind the classification technique is as follows. First, a set of distinct 2-millisecond-long input signals are created from the data-generating process that has been previously described in Section 2.1. For each of these input signals a structural response is recorded under various bolt preload states of interest. For each of these responses AR coefficients are estimated using the above outlined method. The sets of AR coefficients for each damage condition and each input signal forms a training database. Each configuration from a test signal, observed when the system was driven by an input that was not ever observed in the database before (yet came from the same data-generating process as in the original information theoretic context) is classified using these coefficients. A new input signal (created from the same underlying process as the database input signals) is then applied to the structure when the bolt preload level is in an unknown state. Each set of AR coefficients in the training database for the first of the input signals (that is each set of AR coefficients which describe different bolt conditions for the first input signal) is then used to estimate the structural response to the new input signal. One set of coefficients from the training database will minimize the sum of the squared residual errors. The bolt preload state that the structure was in when these AR coefficients were recorded is scored as the “vote” for the unknown bolt condition using that particular input signal. This comparison then takes place for each of the remaining input signals in the training database. This entire process is then repeated using multiple input signals that are imparted to the structure in its unknown bolt preload state. The votes for each bolt condition are then summed and the condition with the plurality of votes is the estimated condition of the bolt preload level.

3. Analytical simulation

This idea was first tested on data generated from a finite element model of a bolted joint. One of the most important objectives that must be achieved when developing numerical finite element models of such a structure is to realistically capture the relevant physical performance characteristics. In this study, it was determined that the effective contact region that exists between overlapping materials in a bolted lap joint was the most essential physical feature that had to be captured in the finite element model. To observe this phenomenon, a high fidelity finite element quarter model of a steel bolt through an aluminum plate was analyzed and then used to quantitatively describe a relation between bolt

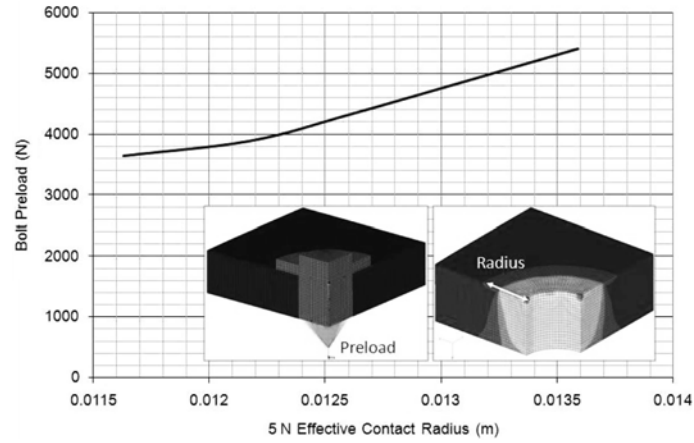


Fig. 6 Numerical bolt preload vs. effective contact radius

preload and effective contact radius. This result can be seen in Fig. 6.

Both the time and space magnitudes of an ultrasonic propagating wave make dynamic transient analysis computationally expensive with commercial off-the-shelf finite element software. Moreover, this computation cost can be substantially increased (by orders of magnitude) with the inclusion of material and geometric nonlinearities like those that exist in our problem. In an effort to mitigate this issue, the most relevant geometric nonlinearity, effective contact between overlapping regions, is encapsulated within several different linear models. Each linear model represented a different bolt preload (effective contact region) state and was analyzed independently with the appropriate input excitation. Fig. 7 illustrates the contact region for each of the bolt preload configurations examined in this study. The elements within the pink region share degrees-of-freedom continuously through the overlapping region of the bars and those outside of the delineation do not.

Using 29 distinct chaotic inputs, response time history data was generated from our detailed finite element models for the 4 simulated bolt preload conditions depicted in Fig. 7. The simulated conditions correspond roughly with a “fully loose” bolt (BO) to “very tight” bolt (FF). Two intermediate preload conditions were also modeled with BP1 representing a looser bolt condition than BP2. A typical input waveform and response time history for two conditions is shown in Fig. 8. It should be noted that the

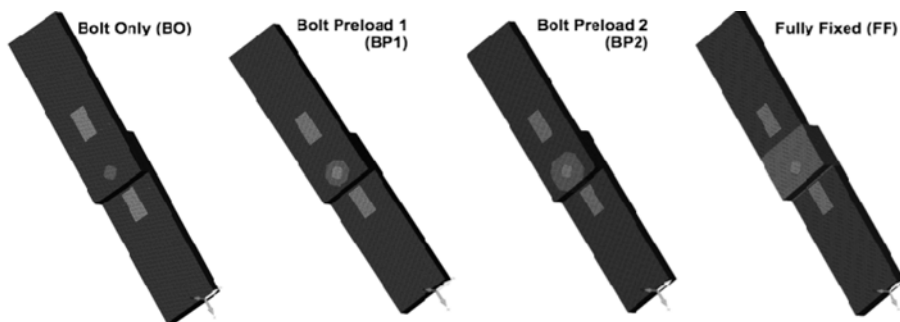


Fig. 7 Depiction of fused surfaces (pink) for all 4 simulated bolt conditions

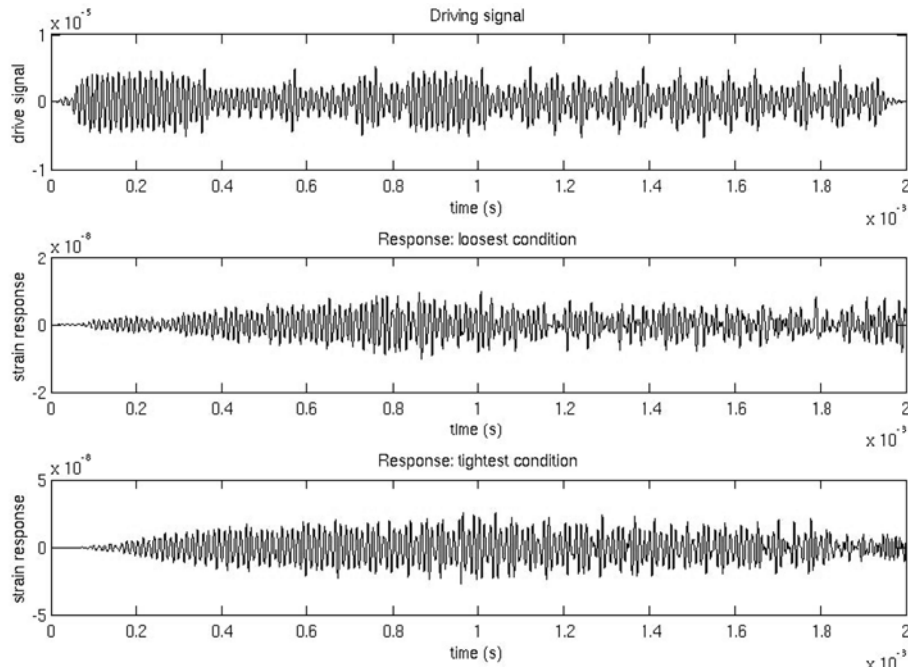


Fig. 8 Simulated CUW input signal (top) and response time history as loosening occurs for BO (middle) and FF (bottom) bolt conditions

“raw” responses shown in the bottom two time series of Fig. 8 do not have any significantly obvious differentiators to the eye.

In order to test the ability of the classification scheme described in Section 2.2 to correctly identify bolt preload condition, 15 of the 29 generated response time histories were selected as database training inputs. The remaining 14 responses were used as test set inputs. All four bolt condition time responses were examined for each of the 14 test inputs. The classification scheme then determined, in each case, the actual bolt condition based solely on knowledge it acquired from the 15 database training inputs. Table 1 shows the summed vote results. Each row represents the actual condition of the bolt and each column is the number of classification votes assigned to that condition. If the statistical classifier correctly identified every test condition the table would only have votes along the diagonal. The correct bolt condition (shown in bold) was able to be identified in all cases. This table shows a strong separation (or lack of confusion) between votes for the correct condition and votes for an incorrect condition with 94% of the individual test cases correctly classifying the ‘true’ bolt condition.

Table 1 Classification “vote” distribution of simulated lap joint data

Actual Condition	Votes				Outcome
	BO	BP1	BP2	FF	
BO	204	0	6	0	Correct
BP1	0	182	28	0	Correct
BP2	0	17	193	0	Correct
FF	0	0	0	210	Correct

4. Experimental investigation

Having shown the strong ability of the damage classification scheme to correctly identify bolt preload state using simulated data, two experimental test platforms were created to test the effectiveness of the method using real materials and the accompanying experimental noise that was not present in simulations. This noise level is minimized to the greatest extent possible by employing shielded cabling as well as moving the test structures an acceptable distance away from the signal amplifier, which emits electromagnetic interference (EMI) during the actuation process. Each input signal is also applied to the structure 50 times and then averaged in a further attempt to reduce experimental noise. The actuation signal is created by the output channel of a National Instruments PCI-6110 DAQ card at a rate of 4 MHz and routed through a Krohn-Hite 7602 wideband power amplifier. This amplified signal is sent to the actuation MFC while the sensing MFC simultaneously samples the structural response at a rate of 4 MHz.

4.1. Single bolt lap joint

The first experimental apparatus on which testing was carried out is the single bolt lap joint shown in Fig. 9. The structure is made up of two aluminum bars ($0.3 \text{ m} \times .05 \text{ m} \times 9.5 \text{ mm}$) connected to each other with a single bolt. Two MFC patches were attached to the structure with one on both sides of the joint. Each of these Smart Material Corp. MFC patches (M 2814 P2) have an active area of $28 \text{ mm} \times 14 \text{ mm}$, are approximately 0.3 mm thick and are bonded to the structure 50 mm from the bolted connection (on each side) using cyanoacrylate. Due to the symmetry of the problem it is not important which patch is used as the sensor and which as the actuator and either configuration will yield similar results. For this experiment the transducer on the left side of the lap joint in Fig. 9 was used as the actuator.

In this study, data were taken at each step of a bolt tightening sequence in which the bolt condition is: 'loose' (Condition 1), 'finger-tight' (Condition 2), 3.5 N-m (Condition 3), and 14 N-m (Condition 4). This sequence is then repeated three times to simulate assembly and disassembly of the joint in a real structure. The first two assembly/disassembly sequences were used to create a training database. Structural responses obtained during the third sequence were used as test inputs. Table 2 shows the vote results for the 4 conditions. Again, if all individual test inputs are classified correctly votes would appear only along the diagonal in bold.

The true bolt condition was correctly assessed by the statistical classification algorithm in all cases but Condition 4 (the most tight), which was estimated by vote-counting to be in Condition 3. There are several factors contributing to this damage case misidentification. First, specifying bolt torque on a real joint can be difficult and in this experiment an inexpensive torque wrench with a fairly low resolution

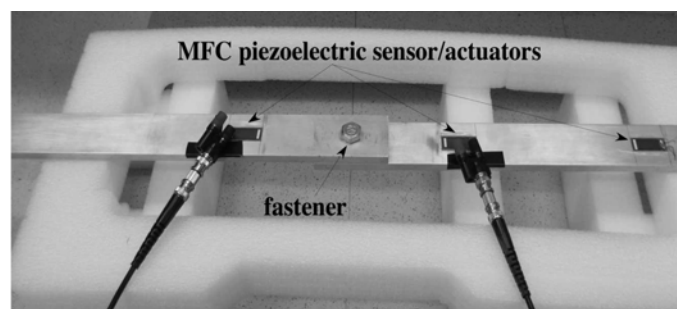


Fig. 9 Single lap joint experiment

Table 2 Classification “vote” distribution of experimental lap joint data

Actual Condition	Votes				Outcome
	Condition 1 (Loose)	Condition 2 (Finger)	Condition 3 (3.5 N-m)	Condition 4 (14 N-m)	
Condition 1 (Loose)	175	46	0	4	Correct
Condition 2 (Finger)	1	150	74	0	Correct
Condition 3 (3.5 N-m)	0	37	188	0	Correct
Condition 4 (14 N-m)	0	24	122	79	Incorrect

was used. Second, the transfer relationship between torque and preload is hysteretic, nonlinear and is highly dependent on local contact, which will vary each time the bolt is tightened. Third, in this experiment it was difficult to maintain the boundary conditions of the lap joint between tests and it is believed that this also led to inflated number of incorrect votes. Given these concerns, the actual preload indicated by a particular torque level may vary significantly from test to test and almost certainly contributed to a much lower percentage of correct identification of individual test cases (66%) than were seen in the simulation results.

In future tests an instrumented bolt will be used so that a direct measure of preload will be available instead of just bolt torque. This should improve results, however in real world situations bolt preload will be specified by torque specifications. Other improvements that are not dependent on knowing exact bolt preload level are possible. Foremost among these are the choice of parameters that affect the creation of the input time signals (carrier frequency f_c , frequency ratio R , modulation depth d) as well as feature extraction (AR model order, size of training and test databases). Using genetic algorithms (specifically differential evolution) to create an optimal input waveform for maximum damage discernment has already been investigated (Fasel, *et al.* 2008). This method showed significant improvement (two orders of magnitude) in solution ‘fitness’ over a random set of input parameters (which is what was used in this study). This statistical classification method has also been used on a composite plate-to-spar bond with multiple disbond sizes as well as a poorly cured bond. Results from these experiments have not yet been published but show that the ability of this method to correctly identify damage state is highly dependent on carrier frequency f_c and frequency ratio R . As well, this classification scheme might be best used, in the case of detecting bolt preload loss, by specifying a critical threshold value of preload level above which the joint is considered healthy and below which the joint is considered damaged. This critical threshold value is further examined in the second experimental structure being investigated in this study.

4.2. Multiple bolt portal structure

As mentioned in the previous section, it is believed that a test bed with more reliable end boundary conditions should result in a greater percentage of correct classifications. It was also desired to test a structure that had multiple bolted connections in order to examine the ability of the statistical classification algorithm to identify multiple damage locations within a structure. This ability to locate damage within a multiple bolt structure is a necessity, as virtually all practical field applications will fall into this category. Therefore, the aluminum frame structure shown in Fig. 10 was employed to address these concerns. The two side bars are the same dimensions as the bars used in the single bolt lap joint experiment (0.3 m × .05 m × 9.5 mm) and the top bar is twice as long (0.6 m × .05 m × 9.5 mm). The actuating MFC is 0.08 m from the close end of the bar (next to bolt 1) and 0.45 m from the far end of

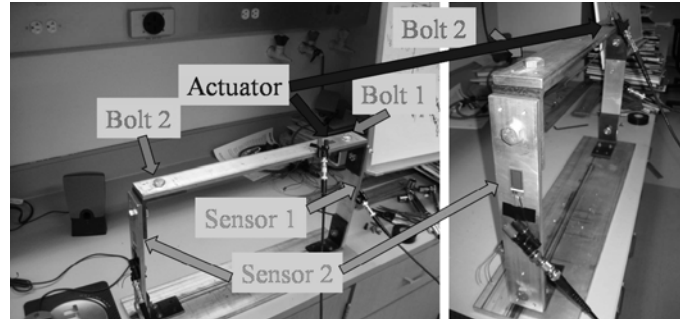


Fig. 10 Multiple joint frame structure experiment

the bar (next to bolt 2). The actuating MFC is placed asymmetrically to remove the symmetry of the structure and to make individual bolt damage state identification more possible. Sensing MFC 1 and MFC 2 are 0.08 m from the top of their respective side bars. The bolts are each 0.4 m from the end of bar.

Table 3 shows the damage cases that were considered in this study. ‘Tight’ indicates 120 in-lb, ‘finger tight’ indicates nominal preload (less than 30 in-lb), and ‘loose’ indicates no preload. While there are thus 7 “conditions” defined, as indicated, there are only 3 damage levels for each bolt. Similar to Section 4.1, the last 7 cases were used as test cases against the training database created using the first 14 cases.

The vote chart for each MFC sensor is shown in Table 4. The bold numbers in each row indicate the

Table 3 Test conditions of the multiple-joint structure

Case	Bolt 1 Condition	Bolt 2 Condition
1	Tight	Tight
2	Finger Tight	Tight
3	Loose	Tight
4	Tight	Finger Tight
5	Tight	Loose
6	Finger Tight	Finger Tight
7	Loose	Loose
8	Tight	Tight
9	Finger Tight	Tight
10	Loose	Tight
11	Tight	Finger Tight
12	Tight	Loose
13	Finger Tight	Finger Tight
14	Loose	Loose
15	Tight	Tight
16	Finger Tight	Tight
17	Loose	Tight
18	Tight	Finger Tight
19	Tight	Loose
20	Finger Tight	Finger Tight
21	Loose	Loose

Table 4 Classification “vote” distribution of multiple-joint frame data

Damage Case	MFC 1 (Bolt 1)			MFC 2 (Bolt 2)		
	Tight	Finger Tight	Loose	Tight	Finger Tight	Loose
15	225	0	0	225	0	0
16	0	152	73	225	0	0
17	2	115	108	225	0	0
18	225	0	0	0	134	91
19	225	0	0	0	98	127
20	1	140	84	0	196	29
21	0	3	222	6	1	224

Table 5 Classification distribution multi-joint experimental data

Damage Case	MFC 1 (Bolt 1)		MFC 2 (Bolt 2)	
	Tight	Loose	Tight	Loose
15	225	0	225	0
16	0	225	225	0
17	2	223	225	0
18	225	0	0	225
19	225	0	0	225
20	1	224	0	225
21	0	225	0	225

true condition of the bolt. Therefore a correct classification is made if the bold number is the largest in its row. As such, the correct classification was made in each case except for bolt 1 in damage case 17. The damage localization ability of this method is still strong as the overall percentage of correctly identified individual test cases is 84%. The ‘tight’ condition was classified correctly for almost every individual test signal. However, the distinction between ‘finger tight’ and ‘loose’ is less clear. This unclear discernability between the ‘finger tight’ and ‘loose’ damage conditions invites the employment of a critical threshold value as discussed in Section 4.1.

Therefore, the categories ‘finger tight’ and ‘loose’ were combined into a more general ‘loose’ category by establishing the critical threshold value at a preload level of ‘finger tight’. In this attempt to make a purely healthy/unhealthy joint status determination, proper classification is achieved with each damage case. This simple classification works so well that votes for individual test responses choose the correct joint configuration greater than 99% of the time, as can be seen in Table 5.

5. Conclusions

This study has shown the structural health monitoring capability of chaotically modulated ultrasonic waves that are imparted to a structure through a piezoelectric patch. The classification damage detection scheme was shown to be effective in identifying bolt preload configuration in simulations and experiments on single and multiple joint structures. This is only one method of identifying structural health using chaotic ultrasonic waves (CUWs). This method has the ability to detect and locate small levels of damage due to the frequency regime of the excitation signal. It will be preferable to standard

ultrasonic SHM techniques that examine dispersion curves, wave attenuation, and reflection characteristics for specific applications because it is easily implemented for complicated geometries.

Future testing will employ the use of an instrumented bolt so that a direct measure of preload will be available instead of just bolt torque. A study that examines optimization of parameters that affect the creation of the input time signals (carrier frequency f_c , frequency ratio R , modulation depth d) as well as feature extraction (AR model order, size of training and test databases) will be undertaken. The use and setting of a critical threshold value of preload level above which the joint is considered healthy and below which the joint is considered damaged is also a future concern. Prior work (Fasel, *et al.* 2006) has shown that similar prediction error metrics can identify very small changes in bolt preload that occur before any structural weakening of the joint is apparent so the critical threshold level should be able to be placed at any level that is needed. A more complex three-dimensional finite element model that can both verify experimental observations and predict simulated damage conditions will also need to be developed.

Acknowledgements

The first author acknowledges partial support through a National Defense Science and Engineering Graduate Research Fellowship. This work was also partially supported through the UCSD/Los Alamos National Laboratory Engineering Institute for Structural Health Monitoring, Damage Prognosis, and Validated Simulations, the Air Force Office of Scientific Research (Dr. Victor Giurgiutiu, Program Manager) and an Air Force Research Laboratory/Missile Defense Agency Joint SBIR contract (Mr. Brandon Arritt, Program Manager).

References

- Abbate, A., Koay, J., Frankel, J., Schroeder, S.C. and Das, P. (1997), "Signal detection and noise suppression using a wavelet transform signal processor: application to ultrasonic flaw detection", *IEEE T. Ultrason. Ferr.*, **44**, 14-26.
- Alleyne, D.N., Lowe, M.J.S. and Cawley, P. (1996), "The inspection of chemical plant pipework using Lamb waves: defect sensitivity and field experience", In: *Review of Progress in Quantitative Nondestructive Evaluation*, Thompson, D.P. and Chimenti, D.E. (eds.), Plenum, New York, 1859-1866.
- Brockwell, P.J. and Davis, R.A. (1991), *Time Series: Theory and Methods*, Springer, New York.
- Bursi, O.S. and Jaspart, J.P. (1998), "Benchmarks for finite element modeling of bolted steel connections", *J. Constr. Steel Res.*, **69**, 361-382.
- Bursi, O.S. and Jaspart, J.P. (1997), "Basic issues in the finite element simulation of extended end plate connections", *Comput. Struct.*, **43**, 17-42.
- Castaigns, M., Cawley, P. and Farlow, R. (1996), "Air-coupled ultrasonic transducers for the detection of defects in plates", In: *Review of Progress in Quantitative Nondestructive Evaluation*, Thompson, D.P. and Chimenti, D.E. (eds.), Plenum, New York, 1083-1090.
- Doebling, S.W., Farrar, C.R., Prime, M.B. and Shevitz, D.W. (1996), "Damage identification and health monitoring of structural and mechanical systems from changes in their vibration characteristics: A literature Review", Los Alamos National Laboratory Report, LA-13070-MS.
- Fasel, T.R., Todd, M.D. and Park, G. (2005), "Piezoelectric active sensing using chaotic excitations and state space reconstruction", *Proc. of the SPIE 10th Annual Int. Symposium on NDE for Health Monitoring and Diagnostics*, **5768**, San Diego, CA, March.
- Fasel, T.R., Todd, M.D. and Park, G. (2006), "Active chaotic excitation for bolted joint monitoring", *Proc. of the*

- SPIE 11th Annual Int. Symposium on NDE for Health Monitoring and Diagnostics*, **6174**, San Diego, CA, March.
- Fasel, T.R., Olson, C.C. and Todd, M.D. (2008), "Optimized guided wave excitations for health monitoring of a bolted joint", *Proc. of the SPIE 13th Annual Int. Symposium on NDE for Health Monitoring and Diagnostics*, **6935**, San Diego, CA, March.
- Giurgiutiu, V. and Zagrai, A. (2002), "Embedded self-sensing piezoelectric active sensors for on-line structural identification", *J. Vib. Acoust.*, **124**, 116-125.
- Giurgiutiu, V. (2005), "Tuned Lamb wave excitation and detection with piezoelectric wafer active sensors for structural health monitoring", *J. Intel. Mat. Syst. Struct.*, **16**, 291-305.
- Guyott, C.H., Cawley, P. and Adams, R.D. (1986), "The non-destructive testing of adhesively bonded structures", *J. Adhesion*, **20**, 129-159.
- Guyott, C.H. and Cawley, P. (1988), "Evaluation of cohesive properties of adhesive joints using ultrasonic spectroscopy", *NDT International*, **21**, 233-240.
- Hess, D.P. (1998), *Vibration and shock-induced loosening*, In: Handbook of Bolts and Bolted Joints, Bickford, J. H. and Nasser S. (Eds.), Marcel Dekker, New York.
- Lanza di Scalea, F., Rizzo, P. and Marzani, A. (2004), "Propagation of ultrasonic guided waves in lapshear adhesive joints: case of incident a0 Lamb wave", *J. Acoust. Soc. Am.*, **115**, 146-156.
- Lowe, M.J.S. and Cawley, P. (1994), "Applicability of plate wave techniques for the inspection of adhesive and diffusion bonded joints", *J. Nondestruct. Eval.*, **13**, 185-200.
- Michaels, J.E. and Michaels, T.E. (2005), "Detection of structural damage from the local temporal coherence of diffuse ultrasonic signals", *IEEE T. Ultrason Ferr.*, **52**, 1769-82.
- Nichols, J.M., Todd, M.D. and Wait, J.R. (2003), "Using state space predictive modeling with chaotic interrogation in detecting joint preload loss in a frame structure experiment", *Smart Mater. Struct.*, **12**(4), 580-601.
- Pai, N.G. and Hess, D.P. (2002), "Experimental study of loosening of threaded fasteners due to dynamic shear loads", *J. Sound Vib.*, **253**, 585-602.
- Pai, N.G. and Hess, D.P. (2002), "Three-dimensional finite element analysis of threaded fastener loosening due to dynamic shear load", *Eng. Fail. Anal.*, **9**, 383-402.
- Pilarski, A. and Rose, J.L. (1992), "Lamb wave mode selection concepts for interfacial weakness analysis", *J. Nondestruct. Eval.*, **11**, 237-249.
- Rokhlin, S.I. (1991), "Lamb wave interaction with lap-shear adhesive joints: theory and experiment", *J. Acoust. Soc. Am.*, **89**, 2758-2765.
- Seifried, R., Jacobs, L.J. and Qu, J. (2002), "Propagation of guided waves in adhesive bonded components", *NDT&E Int.*, **35**, 317-328.
- Shannon, C.E. and Weaver, W. (1949), *The Mathematical Theory of Communication*, Univ. of Illinois Press, Illinois.
- Sohn, H. and Farrar, C.R. (2001), "Damage diagnosis using time series analysis of vibration signals", *Smart Mater. Struct.*, **10**(3), 446-451.
- Sohn, H., Farrar, C.R., Hunter, N.F. and Worden, K. (2001), "Structural health monitoring using statistical pattern recognition", *J. Dyn. Syst. Meas. Control*, **123**, 706-711.
- Staszewski, W.J., Lee, B.C., Mallet, L. and Scarpa, F. (2004), "Structural health monitoring using scanning laser vibrometry: I. Lamb wave sensing", *Smart Mater. Struct.*, **13**(2), 251-260.
- Todd, M.D., Erickson, K., Chang, L., Lee, K. and Nichols, J.M. (2004), "Using chaotic interrogation and attractor nonlinear cross-prediction error to detect fastener preload loss in an aluminum frame", *Chaos: An Interdisciplinary J. Nonlinear Sci.*, **14**(2), 387-399.
- Todd, M.D., Nichols, J.M., Nichols, C.J. and Virgin L.N. (2004), "An assessment of modal property effectiveness in detecting bolted joint degradation: theory and experiment", *J. Sound Vib.*, **275**, 1113-1126.
- Tuzzeo, D. and Lanza di Scalea, F. (2001), "Non-contact air-coupled ultrasonic guided waves for detection of thinning defects in aluminum plates", *Res. Nondestruct. Eval.*, **13**(2), 61-78.
- Wait, J.R., Park, G., Sohn, H. and Farrar, C.R. (2004), "Plate damage identification using wave propagation and impedance methods", *Proc. of the SPIE 9th Annual Int. Symposium on NDE for Health Monitoring and Diagnostic*, **5394**, San Diego, CA, March.
- Wilcox, P.D., Lowe, M.J.S. and Cawley, P. (1999), "Long range Lamb wave inspection: the effect of dispersion

- and modal selectivity”, In: *Review of Progress in Quantitative Nondestructive Evaluation*, Thompson, D. P. and Chimenti, D. E. (eds.), Plenum, New York, 151-158.
- Xu, P.C., Mal, A.K. and Bar-Cohen, Y. (1990), “Inversion of leaky Lamb wave data to determine cohesive properties of bonds”, *Int. J. Eng. Sci.*, **28**, 331-346.